NASA
Technical Memorandum 105567

AVSCOM
Technical Report 91-C-006

Numerical Experiments With Flows of Elongated Granules

Harold G. Elrod
14 Cromwell Court
Old Saybrook, Connecticut

and

David E. Brewe
Propulsion Directorate
U.S. Army Aviation Systems Command
Lewis Research Center
Cleveland, Ohio

Prepared for the
Leeds-Lyon Symposium
Lyon, France, September 3-6, 1991

NASA

US ARMY
AVIATION
SYSTEMS COMMAND

NUMERICAL EXPERIMENTS WITH FLOWS OF ELONGATED GRANULES

H.G. Elrod
14 Cromwell Court
Old Saybrook, Connecticut 06475

and

D.E. Brewe
Propulsion Directorate
U.S. Army Aviation Systems Command
Lewis Research Center
Cleveland, Ohio 44135

Theory and numerical results are given for a program simulating two-dimensional granular flows (1) between two infinite, counter-moving, parallel, roughened walls, and (2) for an infinitely-wide slider. Each granule is simulated by a central repulsive force field ratcheted with force restitution factor to introduce dissipation. Transmission of angular momentum between particles occurs via Coulomb friction. The effect of granule hardness is explored. Gaps from 7 to 28 particle diameters are investigated, with solid fractions ranging from 0.2 to 0.9. Among features observed are: slip flow at boundaries, coagulation at high densities, and gross fluctuations in surface stress.

A videotape has been prepared to demonstrate the foregoing effects.

E-6891

INTRODUCTION:

The purpose of this work is to show how computer simulations of granular flow can assist in the understanding of third-body load support from solid particles. In a literature review conducted several years ago [1] we found that conditions of tribological interest most frequently begin with particle densities greater than those encompassed by the then-current extensions of classical kinetic theory. It was concluded that "simulation programs are a must for third-body tribology." This paper reports on efforts to follow our own recommendation.

In fact, since our review paper, computer simulations have come into increasing use [See ref. 2 for a recent extensive review]. Much of the work has been directed to the mutual confirmation of analytical and numerical methods. This confirmation has been sought through the exploration of regions of overlapping applicability between simulations and earlier analytical results. In particular, constitutive equations have been examined for moderate-density flows of infinite extent, with most of the numerical experiments being performed in three dimensions, and with substantial computer-times being registered.

If suitable constitutive equations can be derived, then appropriate boundary conditions must still be found. Work toward determination of the latter has not been nearly as extensive. In addition, for our purposes, there are at least two other obstacles to overcome. First, in the case of narrow gaps, it is possible that no internal region exists which can be suitably approximated by the constitutive equations for an infinite medium. Second, there must be means for prediction of the large stress and velocity fluctuations which occur. Our purpose in mentioning these difficulties is simply to explain our own choice for a first area of investigation. Certainly for those applications where it is applicable, a successful continuum approach should yield a substantial reduction in the time required for performance calculations, and a greater understanding of the associated flow phenomena. We do recognize the importance of this approach, and hope subsequently to participate in its implementation.

This paper describes our efforts to develop simulation programs for two-dimensional flows. The adoption of this 2-D assumption is tantamount to the assumption of an elongated particle shape, with axis transverse to the flow direction. At this time it is unclear whether typical particles are better approximated by cylinders or by spheres. In the case of wear particles, there is some support for the first alternative. For us, the lower computer time provided by the 2-D assumption was decisive. A much wider range of operating parameters can thereby be explored, and computations are feasible even on a desktop computer. Figure 1 provides a "snapshot" of one flow configuration extensively examined. It consists of two parallel, counter-moving walls of infinite lateral extent separated by a granular medium. In the case of a constant-property Newtonian fluid, the result would be a Couette flow.

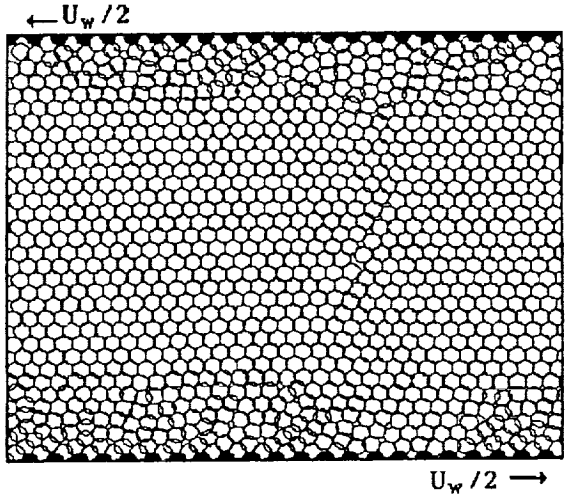

Figure 1 Granular Flow Field Between Infinite Counter-Moving Roughened Parallel Walls 90% solids

Through personal communication we have recently become aware of some research very similar to our own, conducted simultaneously, but independently of us, by S. B. Savage and R. Dai [3,4] (hereinafter referred to as S&D). They have treated bounded simple-shear flows of smooth, inelastic spheres. Their "walls" consisted of massive spheres of the same diameter, spaced to mimic the interior particle distribution. Two different models for interaction were treated, with similar results obtained from each. In one model, the spheres were treated as rigid, with a coefficient of velocity restitution used to introduce dissipation. In the other model, "soft" spheres were used, with dissipation introduced via the Walton "ratchet" model (as also used in this paper). We shall report on some of their findings at the time we discuss our own results.

At the outset, we wish to advise the reader that we do not expect that the kind of investigation reported here will lead to numerically correct predictions of real-life physical systems. Rather, we anticipate that the results will be semi-quantitative, capable of providing important clues to behavior, and a foundation for later empirical representations of real-life experiments.

THEORY

The analysis here will be developed for dissimilar cylinders in contact, although all the reported computations will be for granules of uniform size.

Geometry of Collision:

A granule is taken to be an elongated cylinder of length, L, radius, a, and density, ρ_p. The mass of such a cylinder is:

$$M = \rho_p \pi a^2 L$$

And the moment of inertia of such a granule is:

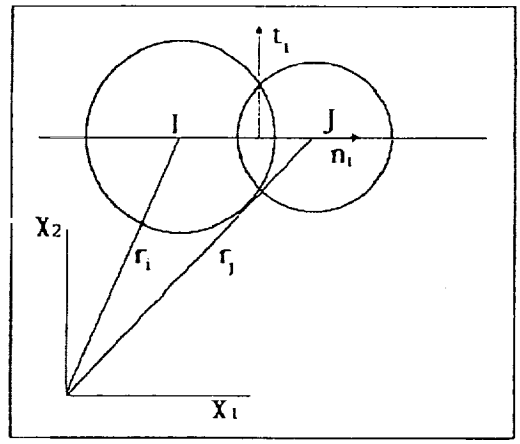

Figure 2 Geometry of Particle-Particle Interaction

$$I = Ma^2/2$$

Figure 2 shows the interaction of two granules, I and J, with radii of a_I and a_J, respectively. For simplicity, we adopt the notation:

$$\underline{\delta r} = \underline{r_j} - \underline{r_i} = \underline{e}_1 \delta x_1 + \underline{e}_2 \delta x_2$$

$r = |\underline{\delta r}|$ = separation of centers

$\underline{n_1} = \underline{\delta r}/r$ = unit normal to point of contact

Expression for Normal Force of Interaction:

The normal separating force exerted by granule J upon granule I (each of length, L) is taken to be:

$$\underline{F_{I,n}} = - \underline{n_1} \; G \; (a_m/a_w) \; \Phi(r/a_m) \; fac$$

Here "G" is a constant force magnitude characteristic of the granular material, "a_w" is the radius of the wall granules, "a_m" is the mean radius of the two interacting granules, Φ is a function to be discussed in a later section, and fac is a factor accounting for energy loss during collision.

During the separation following a collision, fac reduces the repulsive force between the granules. Separation is taking place whenever:

$$\underline{\delta V} \cdot \underline{\delta r} > 0$$

Therefore, we take fac to be:

$$fac = [1 + res - (1 - res)*SGN(\underline{\delta V} \cdot \underline{\delta r})]/2$$

Note that fac = 1 during granule-to-granule approach, and fac = res during separation.

fac is not the coefficient of velocity restitution, res_v. The relationship is (approximately):

$$res_v = \sqrt{fac}$$

Expression for the Tangential Forces:

The tangential force exerted by one cylinder on another during collision can only be represented approximately. We do not account for the deformation which takes place at the surface of the cylinders. Referring to Fig. 2, we take the origin of the vectors $\underline{n}_I$ and $\underline{t}_I$ as the point of contact. The distance from the origin of cylinder, I, to this point is:

$$arm_{IJ} = r/2 + (a_m/r)(a_I - a_J)$$

where: a_I and a_J are the radii of the cylinders I and J, respectively, "r" is the separation of their centers, and

$$a_m = (1/2)(a_I + a_J)$$

Since this expression can lead to preposterous numbers when the cylinder centers are very close, we accept values from the above expression only if they exceed:

$$arm_{IJ}\,(minimum) = a_I - (a_J)^2/(2a_I)$$

Now if the cylinder I is rotating counterclockwise with angular velocity, ω_I, then the local velocity at the so-defined contact point is:

$$\underline{U}_I = \underline{V}_I + \omega_I\,(arm_{IJ}/2)\underline{t}_I$$

The tangent vector, $\underline{t}_I$, is given by:

$$\underline{t}_I = \underline{e}_3 \times \underline{n}_I = (\underline{e}_2\,\delta x_1 - \underline{e}_1\,\delta x_2)/r$$

The tangential component of velocity of particle I relative to particle J at the point of contact is $(\underline{U}_I - \underline{U}_J)\cdot\underline{t}_I$, and is

$$TMT = -\delta\underline{V}\cdot\underline{t}_I + \omega_I\ arm_{IJ} + \omega_J\ arm_{JI}$$

If the above component is positive, then the particle J tends to reduce the angular velocity of particle I. The tangential force exerted by particle J upon particle I is taken to be proportional to the normal repulsive force, with a coefficient of friction, C_f. Thus:

$$\underline{F}_{J,I} = -\,SGN(TMT)\ \underline{t}_I\ C_f\ G\ (a/a_m)\ \Phi(r/a_m)\ fac$$

Equations of Motion:

The equations of motion can now be written:

$$M_I\,(d\underline{V}_I/dt) = \Sigma_J\ (\underline{F}_{J,I} + \underline{F}_{J,I})$$

$$I_I\,(d\omega_I/dt) = \Sigma_J\ arm_{IJ}\ F_{J,I}$$

The summations in these equations account for multi-body collisions.

Non-Dimensional Form:

To reduce as much as possible the number of parameters that must be explored numerically, we put the equations into dimensionless form. We adopt the following

Unit of Distance: a_w
Unit of Time: a_w/U_w
Unit of Mass: M_w

Certain irremovable dimensionless parameters remain in the problem. These are:

1. res, the coefficient of force restitution
2. C_f, the coefficient of friction between particles
3. $f_c = Ga_w/(M_w U_w^2)$
4. (plate separation)$/2a_w = W/2a_w$
5. (separation of roughness particles)$/2a_w$
6. solids fraction
7. parameters used in the dimensionless repulsion function, $\phi(r/a_m)$

Hereafter in this section, dimensionless variables will be employed in the equations. Thus the new $\underline{V}$ will be $\underline{V}/U_w$, the new ω will be $\omega a/U_w$, etc.

The equation for translational motion now becomes:

$$d\underline{V}_I/dt = -\Sigma_I\,F_{rI}\,[\underline{n}_I + \underline{t}_I\,SGN(TMT)\,C_f]$$

and that for rotation:

$$d\omega_I/dt = -\Sigma_I\,F_{rI}\,(M_w/M_I)\ C_f\ SGN(TMT)\,arm_{IJ}$$

where: $F_{rI} = f_c\,(M_w/M_I)(a_m/a_w)\,\phi(r/a_m)\,fac$

and:

$$fac = [1 + res - (1 - res)SGN(TMN)]/2$$

Formula for Repulsive Force:

We revert here to dimensional symbols. The normal force on granule I by granule J has previously been written as:

$$G\,(a_m/a_w)\,\Phi(r/a_m)\ fac$$

In the present study we adopt for Φ a rather arbitrary positive function of the relative separation, r/a_m, with the thought that any generalities concerning granular flow must not depend critically on the details of such a formulation. Certainly this supposition is true in connection with classical kinetic theory of gases. The function chosen for the present investigation is:

$$\Phi(r/a_m) = \exp(-\alpha r/a_m)$$

We define the "force ratio", fr, as the ratio of the repulsive force between wall granules when the center-to-center separation is a_w to that when the separation is $2a_w$ (that is, when the granules are on the verge of no contact). Thus:

$$\alpha = \log_e(fr)$$

This parameter, α, determines how rapidly the repulsive force increases with contact penetration.

Next we choose as a measure of the hardness of the granules the amount of energy required to force an approach from initial contact at $2a_w$ to the separation of a_w. Thus:

$$E = \int_{a_w}^{2a_w} \Phi(r/a_w)\,dr = \frac{[Ga_w(fr-1)]}{[(fr)^2\ln(fr)]}$$

To make this energy non-dimensional, we divide by the kinetic energy of a wall granule moving at velocity, U_w, and form the "hardness ratio", hr. Thus:

$$hr = \frac{2Ga_w}{M_w(U_w)^2}\,\frac{(fr-1)}{(fr)^2\ln(fr)}$$

In the case of two counter-moving walls, we take

$$U_w = U(\text{upper}) - U(\text{lower})$$

As a result of the above definition:

$$f_c = \frac{Ga_w}{M_w(U_w)^2} = \frac{hr}{2}\,\frac{(fr)^2\ln(fr)}{(fr-1)}$$

Collision Time:

To estimate the collision time for a binary encounter, let us assume that granule J is fixed, that granule I is moving solely in the x-direction with initial velocity, U_w, at the commencement of contact (where x is taken as zero). For simplicity, we take both granules to have the same radius, a_w. The motion of granule I is then governed by:

$$du/dt = -(Ga_w/M_wU_w^2)\exp[-\alpha(2-x)]$$

Multiplying top and bottom of the foregoing derivative by "u" and integrating, we get:

$$u^2 = 1 - \beta[\exp(\alpha x) - 1]$$

where:

$$\beta = (2Ga_w/M_wU_w^2)\exp(-2\alpha)$$

The velocity of particle I is reduced to zero at the point:

$$x_{stop} = [\ln(1 + 1/\beta)]/\alpha$$

Now with dt = dx/u, we have for the elapsed time after initial contact:

$$t = \int_0^x \frac{dx}{[1+\beta-\beta\exp(\alpha x)]^{1/2}}$$

This last integration can be accomplished in closed form. Thus:

$$t = (x - 2A/\alpha)/(1+\beta)^{1/2}$$

where:

$$A = \ln[(1+\beta)^{1/2} + \{1+\beta - \beta\exp(\alpha x)\}^{1/2}] - \ln[(1+\beta)^{1/2} + 1]$$

The collision time may be estimated to be roughly twice the time to bring the particle I to a halt. Figure 3 shows the relation between this collision time and the hardness and force ratios. When the force ratio is unity, this time varies inversely with the hardness ratio. The logarithmic scale employed on the chart shows that this relationship is also substantially correct for higher force ratios.

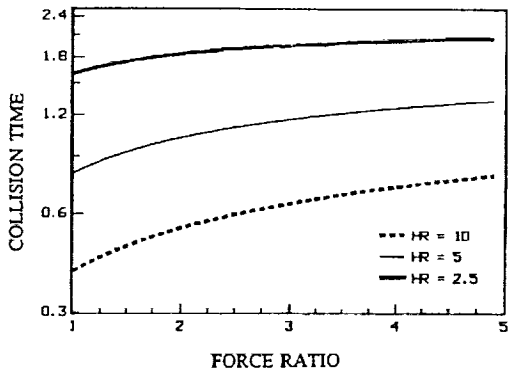

Figure 3 Collision Time as Function of Hardness and Force Ratios

It is important in the numerical calculations that the time-step, Δt, be small enough relative to the collision time for the interaction process to be adequately sampled. Figure 4 shows the effect of the magnitude of Δt on the shear stresses computed for a shear flow between two counter-moving parallel walls separated by a gap of 7 granules diameters with a 50% solids content.

As a result of this Δt-test, the following schedule of Δt was observed in all computations.

HR	Δt
10	0.02
5	0.04
3	0.08

Wall Stresses:

The computations are necessarily performed for a finite computational volume. In the case of parallel walls in relative motion, this volume has width, W (y-direction), length D (x-direction), and depth, L (z-direction, eventually taken as infinite). Particles are affixed to the walls, with spacing close enough so that these particles absorb all the forces exerted on the walls.

Let ΣF denote the sum of forces applied to the particles stretched along one of the walls over length, D. Then the wall stress is

$$\underline{\sigma} = \Sigma \underline{F}/(LD) = \Sigma M_w \underline{a}/(LD)$$

To make the stress non-dimensional, we divide by $\rho_p U_w^2$. Thus:

$$\underline{\sigma}/(\rho_p U_w^2) = \Sigma \pi a_w^2 L \underline{a}/(LDU_w^2) = \pi [\Sigma \underline{a} a_w/U_w^2]/(D/a_w)$$

The righthand side of this last equation involves the non-dimensional acceleration, $\underline{a} a_w/U_w^2$, which the wall particles would possess if unrestrained, as well as the non-dimensional length, D/a_w, of the wall on which the stress is computed.

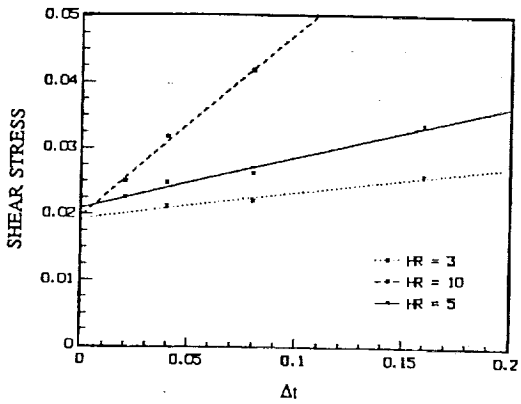

Figure 4 Computed Results for Shear Stress as Function of Δt Employed

NUMERICAL EXPERIMENTS

SHEAR FLOW:

The first numerical experiments were performed on shear flows between counter-moving parallel walls, as shown in Figure 1. The walls were roughened by the attachment of half-cylinders with a center-to-center spacing (unless otherwise stated) of 1.5 diameters. For this configuration, the gap is defined as the center-to-center distance between opposing wall granules. An infinite lengthwise dimension was mimicked by imposition of periodicity in the distribution of granules. The flow computation was commenced by placing granules at random, with zero velocity, within the computational region. In order to attain equilibrium, these granules would repel one another, hitting the walls, and commencing the flow.

Flow quantities were averaged in two stages. In the first stage, quantities were summed and averaged for 50 timesteps. The resultant averages were treated as macroscopic properties, local in time. In the second step, these quantities were averaged over lengthy time periods during which quasi-equilibrium obtained. The time-averaged opposing stresses for the second step were found to match within a few percent. This unforced agreement attests to an accurate implementation of Newton's Laws within the medium. The particle numbers and momenta were also summed and averaged for five equisized slices of the gap. From these data, densities and velocities were computed.

The selection of a desirable time step, Δt, has been discussed. However, the total time to reach a steady-state also must be determined. Inasmuch as the flow never attains a completely steady character, some judgment has to be exercised as to when to terminate the calculations. Although a more rigorous criterion might have been set up (with greater computing time required), the decision for each case was made by examining the transient

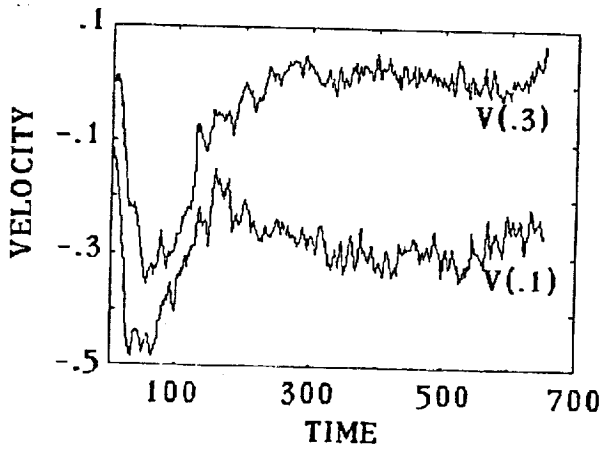

Figure 5 Development of Velocities at 1/10 and 3/10 Across Gap

development. Figure 5 shows such development for the velocities at 0.1 and 0.3 across the gap for the flow shown in Fig. 1. In this particular instance, it would appear sensible to commence averaging for a "final" results at t = 200. Many particles are involved in this computation (1650) and computing time can become excessive. For example, the total runtime for this case was 16.5 hrs. on an IBM (clone) 486 33. This computer runs approximately 36 times as fast as the original IBM AT.

With so many parameters assignable for the investigation, some choices had to be made. The effect of granule hardness was explored with a gap of 7 diams. Figure 6 shows that shear stresses at densities below 60% are virtually independent of HR. This result is in keeping with classical kinetic theory of gases, where different molecular models tend to give similar results. It is, moreover, in agreement with the finding of S&D of similar results for rigid and soft granules. Above 60% solids, our values rise rapidly, and at rigid-body complete filling (90.7%), they are proportional to HR.

In all further discussion, unless specifically stated otherwise, the following values were assigned for the numerical computations.

HR = 5, FR = 3, res = .8, CF = .3
Ctr.-to-Ctr. Spacing of Wall Particles, 1.5

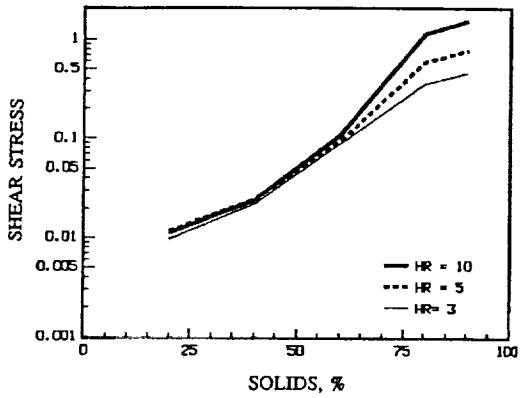

Figure 6 Shear Stress Dependence on Hardness Ratio and Density

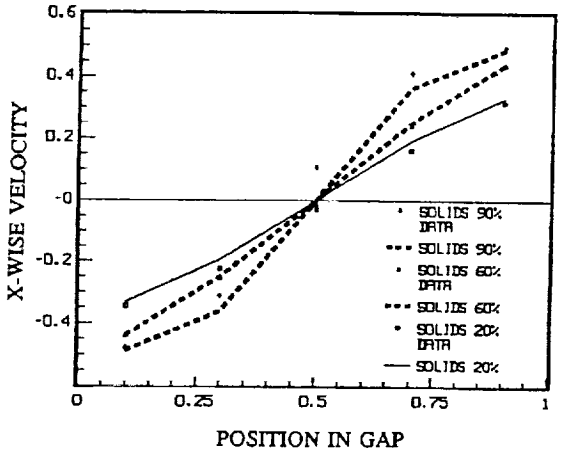

Figure 7 Velocity Distribs. for 7 Diam. Gap HR = 5; FR = 3; CF = 0.3; res = 0.8

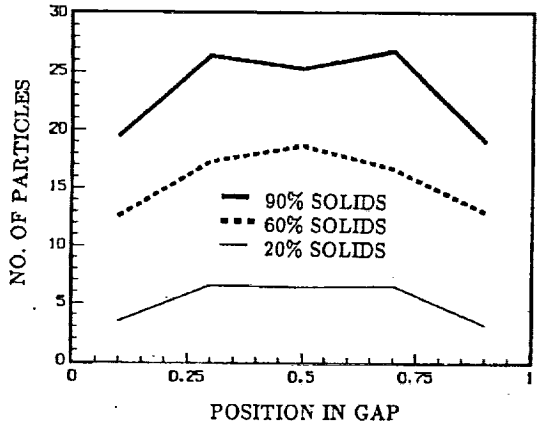

Figure 8 Particle-Count Density Distribution for 7 Diam. Gap

Figures 7 and 8 show the velocity and particle distributions obtained for a gap of 7 diams. Antisymmetry was forced on the velocity profiles, with the supporting points shown as data. At low density, the velocity distribution is typical Couette Flow, with slip at the walls. With increasing density, the velocity gradient tends to be steeper in the interior than it is near the walls, and the slip approaches zero (as found also by S&D). The density distributions are only for the "active" or unattached granules. Near the wall the available space for such active granules is restricted, and the effective density is augmented by the inclusion of the half-cylinders (in this case making an addition of 5).

Figures 9 and 10 show the velocities and densities for a gap of 28 diams. At low densities, the Couette Flow with slip is again observed. However, in contrast with the small gap case, the interior velocity gradient diminishes with increasing granule density. In the high density limit, a plug is formed within the interior, the particle aggregate becoming effectively a solid. This phenomenon is clearly visible in Figure 1, where the granules are lined up within the interior, and ruffled in the regions adjacent to the walls. The density distribution shows a slight trough in the center of the gap.

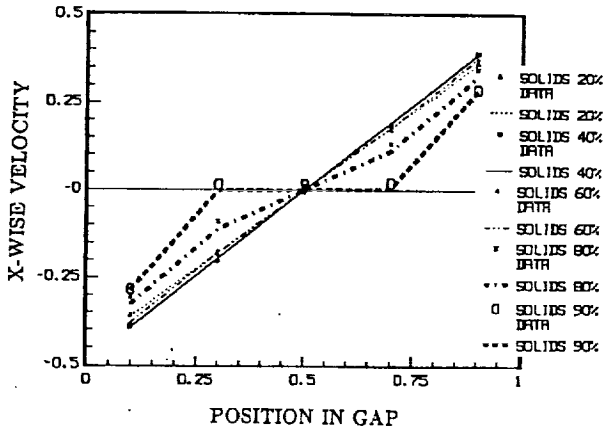

Figure 9 Velocity Dist. for 28 Diam. Gap HR = 5; FR = 3; CF = 0.3; res = 0.8

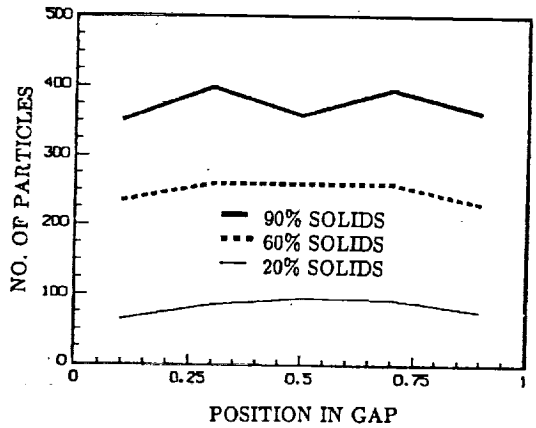

Figure 10 Particle-Count Density Dist. for 28 Diam. Gap

The corresponding results for a gap of 14 diams. have been computed, and found to lie between those for 7 and 28 diameters. The lining up of particles, as observed in Figure 1, is an extreme example of the "layering" reported by S&D. These investigators also

report that with a 7 diam. gap, the interior flow stresses agree reasonably well with extended kinetic theories. They do not give, however, results for greater gaps, where we find a trend away from the smaller gap behavior. It is pertinent to observe at this juncture that computer simulations of an infinite flow field do, by the very manner in which they mimic infinity in the direction transverse to the flow, tend to deny the possibility of flow coagulation.

The reader will have observed that the higher-density velocity data do not necessarily support an antisymmetric profile. Whereas at low densities, when the same gross boundary conditions are applied, all initial particle distributions appear to lead to the same mean flow, the same cannot be uneqivocally stated for higher densities. Lack of antisymmetry and of reproducibility has been observed. Further study should be made of this matter. S&D also report similar findings.

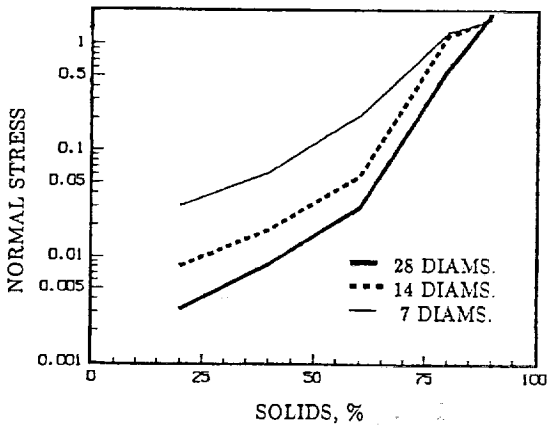

Figure 11 Dependence of Normal Stress on Solids % and Gap

The dependence of the normal stress on gap and solids content is shown in Figure 11. At low densities this stress varies nearly inversely to the gap. On the other hand, at the upper density limit, the stress is generated almost totally by compression, and is independent of gap size. The corresponding values of the overall friction coefficient, shear/normal stress, are shown in Figure 12. There is a change in behavior with gap size. The curve for the largest gap exhibits the minimum observed for infinite media.

To determine the influence of the internal friction coefficient, CF, runs were made with a gap of 7 diams. Figure 13 shows the significant, but not dramatic, difference between the results for CF = 0 and CF = 0.3.

"SLIDER BEARING":

The second case treated numerically was an inclined "slider bearing" [For a discussion of this case, see ref. 5]. A uniform layer of granules is drawn by a moving plate into the wedge formed by that plate and another, of finite length, inclined to it. Figure 14 shows

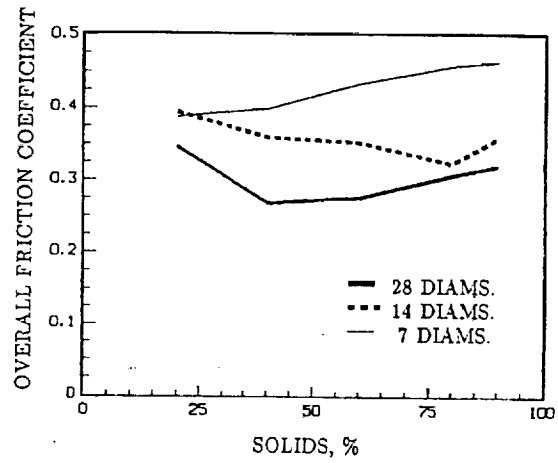

Figure 12 Overall Friction Coefficient as Function of Solids % and Gap

the "slider" with an inlet gap of 20 granule diameters, an exit gap of 10 diams., and a total length of 20 diams. In every case, the thickness of the oncoming layer is such that it just fits into the exit gap, H2 (thus a thickness of 4 for an exit H2 = 5).

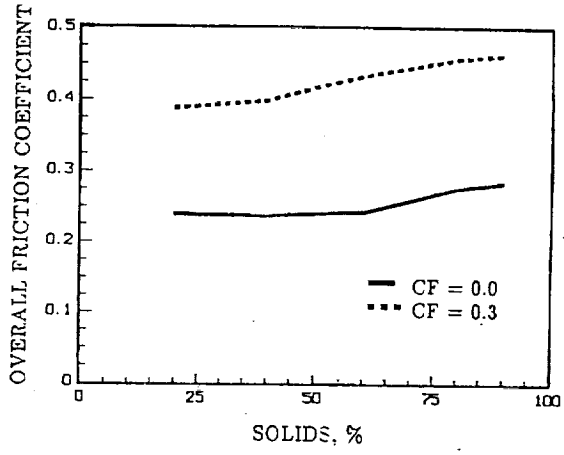

Figure 13 Dependence of Overall Friction Coeff.on Friction Coeff. between Granules

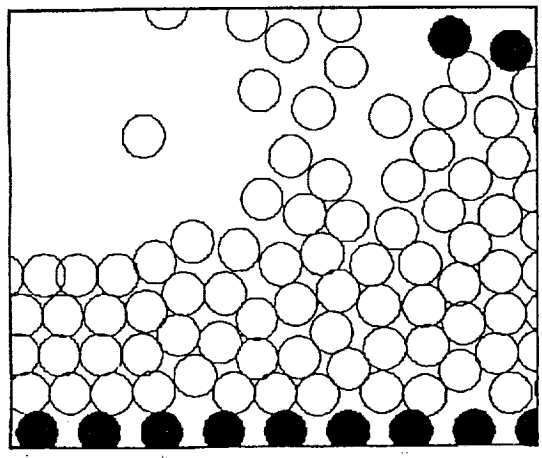

Figure 14 Entrance Region of "Slider" with H1 = 10 Diam. & H2 = 5 Diam.

Figure 14 shows the entrance region. We see the particles rejected backwards as the slider plows its way over the oncoming carpet

slider plows its way over the oncoming carpet of granules. In Fig. 15 we see granules burst out from the compression experienced in the tight gap. The velocity profiles at entrance, midway and exit are shown in Figure 16. They resemble those to be found in a classical, liquid-lubricated flat slider bearing.

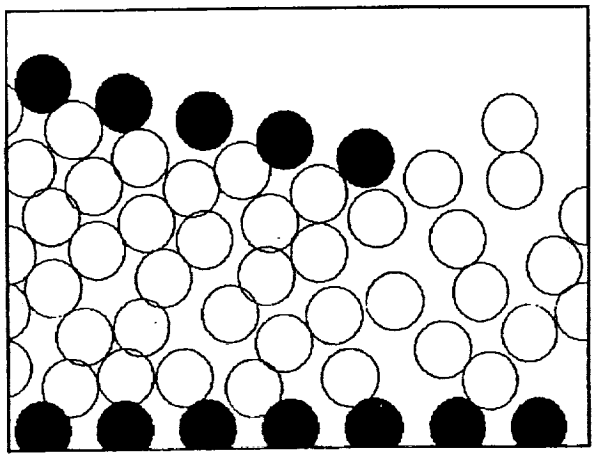

Figure 15 Exit Region of Slider with H1 = 10 Diam. & H2 = 5 Diam.

The force distribution exerted by the granules upon the slider was not calculated, but the relative total longitudinal and vertical forces were determined, as given below.

Configuration H1	H2	D	FX	FY
10	5	10	2.58	4.00
10	5	20	3.94	8.11
8	8	10	2.36	4.46

The significant result here is that, within the range of parameters investigated, the load capacity does not depend on the slider inclination. Thus, although the velocity profiles may resemble those of classical lubrication, the load-carrying capacity does not.

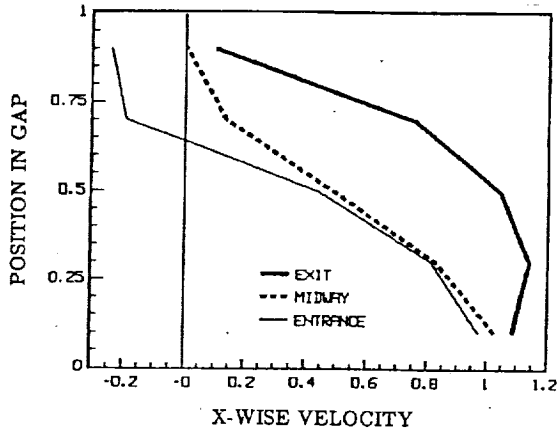

Figure 16 Velocity Dist. within "Slider" with H1 = 10 Diam. & H2 = 5 Diam

BIBLIOGRAPHY:

1. *Granular Flow as a Tribological Mechanism -- a First Look*, H. G. Elrod, Leeds-Lyon Symposium, Sept. 1987.

2. *Rapid Granular Flows*, C. S. Campbell, *Ann. Rev. Fluid Mech.*, vol. 22, pp. 57-92, 1990, Annual Reviews, Inc., Palo Alto, CA.

3. *Numerical Simulations of Couette Flow of Granular Materials; Spatio-Temporal Coherence and 1/f Noise*, S. B. Savage, *Physics of Granular Media*, ed. J. Dodds & D. Bideau, Nova Scientific Press, New York, June 1991.

4. *Some Aspects of Bounded and Unbounded Shear Flows of Granular Material*, S. B. Savage & R. Dai, U. S.-Japan Meeting, Clarkson Univ., U. S. A., Aug. 4-10, 1991.

5. *Mechanismes et Tribolgie*, Yves Berthier, These presentee devant L'Institut National des Sciences Appliquees de Lyon et L'Universite Claude Bernard de Lyon, France, 1988.

REPORT DOCUMENTATION PAGE

Form Approved
OMB No. 0704-0188

1. AGENCY USE ONLY (*Leave blank*)	2. REPORT DATE	3. REPORT TYPE AND DATES COVERED
	1992	Technical Memorandum

4. TITLE AND SUBTITLE

Numerical Experiments With Flows of Elongated Granules

5. FUNDING NUMBERS

WU-505-62-0K
1L161102AH45

6. AUTHOR(S)

Harold G. Elrod and David E. Brewe

7. PERFORMING ORGANIZATION NAME(S) AND ADDRESS(ES)

NASA Lewis Research Center
Cleveland, Ohio 44135-3191
and
Propulsion Directorate
U.S. Army Aviation Systems Command
Cleveland, Ohio 44135-3191

8. PERFORMING ORGANIZATION REPORT NUMBER

E-6891

9. SPONSORING/MONITORING AGENCY NAMES(S) AND ADDRESS(ES)

National Aeronautics and Space Administration
Washington, D.C. 20546-0001
and
U.S. Army Aviation Systems Command
St. Louis, Mo. 63120-1798

10. SPONSORING/MONITORING AGENCY REPORT NUMBER

NASA TM-105567
AVSCOM-TR-91-C-006

11. SUPPLEMENTARY NOTES

Prepared for the Leeds-Lyon Symposium, Lyon, France, September 3-6, 1991. Harold G. Elrod, Consultant, 14 Cromwell Court, Old Saybrook, Connecticut 06475; David E. Brewe, Propulsion Directorate, U.S. Army Aviation Systems Command. Repsonsible person, David E. Brewe, (216) 433-6067.

12a. DISTRIBUTION/AVAILABILITY STATEMENT

Unclassified - Unlimited
Subject Category 37

12b. DISTRIBUTION CODE

13. ABSTRACT (*Maximum 200 words*)

Theory and numerical results are given for a program simulating two-dimensional granular flows (1) between two infinite, counter-moving, parallel, roughened walls, and (2) for an infinitely-wide slider. Each granule is simulated by a central repulsive force field ratcheted with force restitution factor to introduce dissipation. Transmission of angular momentum between particles occurs via Coulomb friction. The effect of granule hardness is explored. Gaps from 7 to 28 particle diameters are investigated, with solid fractions ranging from 0.2 to 0.9. Among features observed are: slip flow at boundaries, coagulation at high densities, and gross fluctuations in surface stress. A videotape has been prepared to demonstrate the foregoing effects.

14. SUBJECT TERMS

Granular materials; Powder; Particles; Solid lubricants; Numerical flow visualization; Numerical analysis; Kinetic energy; Kinetic equations; Shear flow

15. NUMBER OF PAGES

10

16. PRICE CODE

A02

17. SECURITY CLASSIFICATION OF REPORT	18. SECURITY CLASSIFICATION OF THIS PAGE	19. SECURITY CLASSIFICATION OF ABSTRACT	20. LIMITATION OF ABSTRACT
Unclassified	Unclassified	Unclassified	